Dynamic properties of one-component strongly coupled plasmas: The sum-rule approach

Yu. V. Arkhipov,[1] A. Askaruly,[1] D. Ballester,[2] A. E. Davletov,[1] I. M. Tkachenko,[3] and G. Zwicknagel[4]
[1]*Department of Optics and Plasma Physics, Al-Farabi Kazakh National University, Tole Bi 96, Almaty 050012, Kazakhstan*
[2]*School of Mathematics and Physics, Queen's University, Belfast BT7 1NN, United Kingdom*
[3]*Instituto de Matemática Pura y Aplicada, Universidad Politécnica de Valencia, Camino de Vera s/n, 46022 Valencia, Spain*
[4]*Institut für Theoretische Physik II, Erlangen-Nürnberg Universität, Staudtstr. 7, D-91058 Erlangen, Germany*
(Received 13 November 2009; published 8 February 2010)

The dynamic characteristics of strongly coupled one-component plasmas are studied within the moment approach. Our results on the dynamic structure factor and the dynamic local-field correction satisfy the sum rules and other exact relations automatically. A quantitative agreement is obtained with numerous simulation data on the plasma dynamic properties, including the dispersion and decay of collective modes. Our approach allows us to correct and complement the results previously found with other treatments.

DOI: 10.1103/PhysRevE.81.026402 PACS number(s): 52.27.Aj, 52.27.Gr

I. INTRODUCTION

The classical one-component plasma (OCP) might be considered a test-tube for the modeling of strongly interacting Coulomb systems [1], see also [2,3] for more recent reviews. OCP is often employed as a simplified version of real physical systems ranging from electrolytes and charged-stabilized colloids [4], laser-cooled ions in cryogenic traps [5] to dense astrophysical matter in white dwarfs and neutron stars [6]. Another modern and highly interesting pattern of the OCP is dusty plasmas with the pure Coulomb interparticle interaction potential substituted by the Yukawa effective potential [7].

The classical OCP is defined as a system of charged particles (ions) immersed in a uniform background of opposite charge. It is characterized by a unique dimensionless coupling parameter

$$\Gamma = \beta(Ze)^2/a. \tag{1}$$

Here β^{-1} stands for the temperature in energy units, Ze designates the ion charge, and $a=(3/4\pi n)^{1/3}$ is the Wigner-Seitz radius, n being the number density of charged particles. For $\Gamma \gtrsim 1$ the interaction effects determine the physical properties of the OCP.

The OCP static properties like the pair correlation function, $g(r)$, the static structure factor (SSF), $S(k)$, and the static local-field correction, $G(k)$, can be found by computer simulations (see [2,3]). Moreover, molecular dynamics (MD) as well as other simulations can provide valuable information on the dynamic structure factor (DSF), $S(k,\omega)$, and other dynamic characteristics.

In this paper, the OCP dynamic properties are studied by the moment approach based on sum rules and other exact relations, see [8,9] and references therein and comparison is made with the simulation data of Hansen *et al.* [10] and of Wierling *et al.* [3]. The results of alternative theoretical methods, the quasilocalized charge approximation (QLCA) [2,11,12], the viscoelastic approximation (VEA) [13,14], and the recurrence relation (RR) technique [3,15], are considered as well.

Precisely, the aim of the work is threefold. First, we use the method of moments to study the OCP dispersion plasmon frequency, $\omega_L(k)$, the corresponding decay decrement, $\delta_L(k)$, and the dynamic local-field correction (DLFC), $G(k,\omega)$. Second, we compare our results on the dynamic structure factor to the MD simulation data of [10] and pay special attention to onset of the so-called negative dispersion of the plasmon mode in strongly coupled OCPs by determining the range of the coupling parameter Γ within which the derivative $d\omega_L(k)/dk$ changes its sign. And third, we crosscheck our results against the theoretical methods mentioned above. In particular, we note that the plasmon decay rate cannot be studied within the QLCA approach due to its intrinsic nature and its k dependence was not referred to in the literature as yet. We also show how the VEA and RR results for the DLFC and the DSF can be retrieved and partly extended within the sum rule or moment approach.

II. MATHEMATICAL BACKGROUND

Consider five convergent sum rules which are frequency power moments of the system DSF,

$$S_\nu(k) = \frac{1}{n}\int_{-\infty}^{\infty} \omega^\nu S(k,\omega)d\omega, \quad \nu = 0,1,2,3,4. \tag{2}$$

All odd-order moments vanish since, in a purely classical system, the DSF is an even function of frequency.

The method of moments is, generally speaking, capable of handling any number of convergent sum rules. In two-component plasmas, though, all higher-order frequency moments diverge which can be attributed to and understood [16] from the exact asymptotic form of the imaginary part of the dielectric function [17]. There is no such clear theoretical result for the model system to be dealt with here and, thus, it is simply impossible to presume that the three first even order moments [Eq. (2)] are the only convergent even order frequency sum rules. However, the ambiguity of higher-order

frequency moments [13], related to our scarce knowledge of the triplet and, presumably, higher-order correlation functions, remains insuperable nowadays and can only impede our understanding of the physical processes to be described below.

It is well known [18] that the analytic prolongation of the positive function of frequency, DSF, onto the upper half plane Im $z>0$, constructed by means of the Cauchy integral formula,

$$S(k,z)=\frac{1}{n}\int_{-\infty}^{\infty}\frac{S(k,\omega)}{\omega-z}d\omega, \tag{3}$$

admits the asymptotic expansion

$$S(k,z\to\infty)\simeq-\frac{S_0(k)}{z}-\frac{S_2(k)}{z^3}-\frac{S_4(k)}{z^5}-\mathrm{o}\left(\frac{1}{z^5}\right),\quad \mathrm{Im}\,z\geq 0. \tag{4}$$

The zero-order moment is, obviously, the SSF, $S_0(k)=S(k)$, while the second moment is the f-sum rule,

$$S_2(k)=\omega_0^2(k)=\omega_p^2\left(\frac{k^2}{k_D^2}\right)=\omega_p^2\left(\frac{q^2}{3\Gamma}\right), \tag{5}$$

and

$$S_4(k)=\omega_p^2\omega_0^2(k)\left\{1+\frac{3k^2}{k_D^2}+U(k)\right\}=\omega_p^2\omega_0^2(q)\left\{1+\frac{q^2}{\Gamma}+U(q)\right\}. \tag{6}$$

Here $q=ka$, $\omega_p=\sqrt{4\pi ne^2/m}$ refers to the plasma frequency, and $k_D=\sqrt{4\pi ne^2Z^2\beta}$ is the Debye wavelength, m being the ion mass, and

$$U(q)=\frac{1}{4\pi^2 n}\int_0^{\infty}[S(k')-1]f(k';k)k'^2dk'=\frac{1}{3\pi}\int_0^{\infty}[S(p)-1]f(p;q)p^2dp,$$

where

$$f(p;q)=\frac{5}{6}-\frac{p^2}{2q^2}+\left(\frac{p^3}{4q^3}-\frac{p}{2q}+\frac{q}{4p}\right)\ln\left|\frac{q+p}{q-p}\right|,\quad q=ka,$$

$$p=k'a.$$

This last contribution to the fourth moment is due to the ion-ion interactions in the OCP, while the second term represents the Vlasov correction to the ideal-gas dispersion relation of the plasmon mode, $\omega_L=\omega_p$.

As in [19] the following limits hold

$$U(k\to\infty)=\frac{2}{3}(g(0)-1)=-\frac{2}{3}, \tag{7}$$

$$U(k\to 0)\simeq\frac{2}{15}\frac{\langle\phi(k)\rangle}{\phi(k)}, \tag{8}$$

where, by virtue of Parseval's theorem,

$$\langle\phi(k)\rangle=\int\phi(k)[S(k)-1]\frac{d\mathbf{k}}{(2\pi)^3n}=\int\phi(r)[g(r)-1]d\mathbf{r}$$

is the average interaction energy between two ions with

$$\phi(k)=4\pi(Ze)^2/k^2,\quad \phi(r)=(Ze)^2/r.$$

The Nevanlinna formula of the classical theory of moments [18,20] expresses the response function [8]

$$S(k,z)=-\frac{1}{n}\frac{E_3(z;k)+Q(k,z)E_2(z;k)}{D_3(z;k)+Q(k,z)D_2(z;k)} \tag{9}$$

in terms of a Nevanlinna class function $Q=Q(k,z)$, analytic in the upper half-plane Im $z>0$ with a positive imaginary part: Im $Q(k,\omega+i\eta)>0$, $\eta>0$. The function $Q(k,z)$ should additionally satisfy the limiting condition:

$$\frac{Q(k,z)}{z}\underset{z\uparrow\infty}{\to}0,\quad \mathrm{Im}\,z>0. \tag{10}$$

Any such function admits the integral representation [18,20]

$$Q(k,z)=\frac{i}{\tau(k)}+2z\int_0^{\infty}\frac{du(t)}{t^2-z^2} \tag{11}$$

with $\tau(k)>0$ and a nondecreasing bounded function $u(t)$ such that

$$\int_{-\infty}^{\infty}\frac{du(t)}{1+t^2}<\infty.$$

Furthermore, the polynomials $D_j(z;k)$, $j=0,1,2,3$, orthogonal with respect to the distribution density $S(k,\omega)$ [21] together with their conjugate counterparts $E_j(z;k)$, $j=0,1,2,3$ determined as

$$E_j(z;k)=\int_{-\infty}^{\infty}\frac{D_j(\omega;k)-D_j(z;k)}{\omega-z}S(k,\omega)d\omega,\quad j=0,1,2,3$$

have real coefficients and their real zeros simply alternate [18,20]. A rather routine renormalization casts these polynomials as

$$D_0(z;k)=1,\quad D_1(z;k)=z,\quad D_2(z;k)=z^2-\omega_1^2(k),$$

$$D_3(z;k)=z^3-z\omega_2^2(k),\quad E_0(z;k)\equiv 0,\quad E_1(z;k)=S_0(k),$$

$$E_2(z;k)=S_0(k)z,\quad E_3(z;k)=S_0(k)[z^2+\omega_1^2(k)-\omega_2^2(k)]. \tag{12}$$

The frequencies $\omega_1(k)$ and $\omega_2(k)$ in Eq. (12) are defined by the respective ratios of the moments $S_\nu(k)$ [8] and, thus, are determined by the system static characteristics:

$$\omega_1^2=\omega_1^2(k)=S_2(k)/S_0(k),\quad \omega_2^2=\omega_2^2(k)=S_4(k)/S_2(k). \tag{13}$$

The DSF is therefore found from Eq. (3) as

$$S(k,\omega)=\frac{n}{\pi}\lim_{\eta\downarrow 0}\mathrm{Im}\,S(k,\omega+i\eta)=\frac{n}{\pi}\frac{S(k)\omega_1^2(\omega_2^2-\omega_1^2)\mathrm{Im}\,Q(k,\omega)}{[\omega(\omega^2-\omega_2^2)+\mathrm{Re}\,Q(k,\omega)(\omega^2-\omega_1^2)]^2+[\mathrm{Im}\,Q(k,\omega)]^2(\omega^2-\omega_1^2)^2}. \tag{14}$$

In the present work we *approximate* the Nevanlinna interpolation function $Q(q,z)$ by its *static value* $i\tau^{-1}(k)=Q(k,0)$, where the "relaxation time" is selected to reproduce an exact static value of the dynamic structure factor in Eq. (14):

$$\tau(k)=\frac{\pi S(k,0)}{nS(k)}\frac{\omega_1^2(k)}{\omega_p^2\Delta(k)}. \tag{15}$$

Alternatives in determination of the relaxation time were discussed in [22] (Chap. 9). Note that

$$\Delta(k):=\frac{\omega_2^2(k)-\omega_1^2(k)}{\omega_p^2}>0 \tag{16}$$

due to the Cauchy-Schwarz inequality. It is important that the DSF [Eq. (14)], by virtue of Eq. (10), obeys the correct asymptotic expansion (4) and, hence, satisfies the sum rules (2) by construction, regardless of the form of the Nevanlinna parameter function $Q(k,z)$. On the other hand, this means that the asymptotic expansion (4) holds for any adequate choice of the function $Q(k,z)$.

Within the approximation described above we adopt

$$\frac{S(k,\omega)}{S(k,0)}=\frac{\omega_1^4}{[\omega^2-\omega_1^2(k)]^2+[(\omega^2-\omega_2^2(k))\omega\tau(k)]^2}. \tag{17}$$

The static characteristics, i.e., $S(k,0)$, $S(k)$ together with the moments $S_2(k)$ and $S_4(k)$, which, in turn, determine the characteristic frequencies $\omega_1(k)$, $\omega_2(k)$, and $\tau^{-1}(k)$, are to be calculated independently, e.g., in the hypernetted chain (HNC) approximation or to be taken directly from the MD simulation data on the DSF. Straightforward comparison of the data obtained from Eq. (17) with the simulation data is transferred to Sec. V. Note that the DSF [Eq. (17)] contains an exact static value, $S(k,0)$.

In a classical system and due to the fluctuation-dissipation theorem (FDT),

$$S(k,\omega)=\frac{\mathcal{L}(k,\omega)}{\pi\beta\phi(k)} \tag{18}$$

so that the moments [Eq. (2)] are proportional, for a given value of the wave number, to the corresponding moments of the loss function

$$\mathcal{L}(k,\omega)=-\frac{\mathrm{Im}\,\epsilon^{-1}(k,\omega)}{\omega}, \tag{19}$$

in the following way:

$$S_\nu(k)=\frac{k^2}{k_D^2}C_\nu(k),\quad \nu=0,2,4, \tag{20}$$

$$C_\nu(k)=\frac{1}{\pi}\int_{-\infty}^{\infty}\omega^\nu\mathcal{L}(k,\omega)d\omega,\quad \nu=0,2,4. \tag{21}$$

where $\epsilon^{-1}(k,\omega)$ stands for the plasma inverse dielectric function (IDF), a genuine response (Nevanlinna) function of frequency.

Since the DSF has previously been constructed on the basis of the Nevanlinna formula [18,20], we, thus, obtain for the IDF [8]:

$$\epsilon^{-1}(k,z)=1+\frac{\omega_p^2(z+Q)}{z(z^2-\omega_2^2)+Q(z^2-\omega_1^2)},\quad z=\omega+i0^+, \tag{22}$$

where, the Nevanlinna parameter function $Q=Q(k,z)$ coincides with that of Eq. (9) due to relation (18). The main objective of the following section is to compare expression (17) to those stemming from the viscoelastic approximation [13,14] and the continued-fraction approach.

III. ALTERNATIVE THEORETICAL APPROACHES

A. VEA

It is well known that the VEA is based on the random-phase approximation (RPA) for the polarization operator and interpolates between the DLFC and the RPA itself [14]. Consider, first, the RPA polarization operator (a simple loop)

$$\Pi(k,\omega)=\beta n[1+\zeta Z(\zeta)],\quad \zeta=\frac{\omega}{k}\sqrt{\frac{\beta m}{2}}+i0^+.$$

Here

$$Z(\zeta)=\frac{1}{\sqrt{\pi}}\int_{-\infty}^{\infty}\frac{\exp(-t^2)}{t-\zeta}dt \tag{23}$$

is the plasma dispersion function [23]. Note that the following expansions hold:

$$Z(\zeta\to 0)\simeq i\sqrt{\pi}\exp(-\zeta^2)-2\zeta\left(1-\frac{2}{3}\zeta^2+\frac{4}{15}\zeta^4-\cdots\right), \tag{24}$$

$$Z(\zeta\to\infty)\simeq i\sqrt{\pi}\exp(-\zeta^2)-\zeta^{-1}\left(1+\frac{1}{2\zeta^2}+\frac{3}{4\zeta^4}+\cdots\right). \tag{25}$$

When the coupling effects come to play, the DLFC amends the RPA form of the IDF as follows:

$$\epsilon^{-1}(k,\omega)=1-\frac{\phi(k)\Pi(k,\omega)}{1-\phi(k)[G(k,\omega)-1]\Pi(k,\omega)}. \tag{26}$$

A direct comparison of Eqs. (22) and (26) leads to the following expression for the DLFC:

$$G(k,\omega) = A(k,\omega) + \frac{\Delta(k)}{1 + \dfrac{\omega}{Q(k,\omega)}}, \tag{27}$$

which, in the static approximation $Q(k,\omega) = i\tau^{-1}(k)$ we employ, simplifies to

$$G(k,\omega) = A(k,\omega) + \frac{\Delta(k)}{1 - i\tau\omega} = \frac{B(k,\omega) - i\tau\omega A(k,\omega)}{1 - i\tau\omega}. \tag{28}$$

Right above the following notations are utilized:

$$A(k,\omega) = 1 + \frac{1}{\phi(k)\Pi(k,\omega)} + \frac{\omega^2 - \omega_2^2}{\omega_p^2},$$

$$B(k,\omega) = A(k,\omega) + \Delta(k).$$

Due to the Kramers-Kronig relation,

$$\epsilon^{-1}(k,\omega) = 1 - \frac{1}{\pi}\int_{-\infty}^{\infty} \mathcal{L}(k,\omega')\frac{\omega' d\omega'}{\omega' - z}, \quad z = \omega + i0^+, \tag{29}$$

$$S(k) = S_0(k) = \frac{k^2}{k_D^2}C_0(k) = \frac{k^2}{k_D^2}[1 - \epsilon^{-1}(k,0)] \tag{30}$$

so that the correct value of the static local-field correction (SLFC), $B(k,0) = G(k,0) \coloneqq G(k)$ is automatically obtained from Eq. (27). Moreover, by virtue of Eq. (30), the SLFC is directly related to the SSF:

$$G(k) = 1 + \frac{k^2}{k_D^2}\left[1 - \frac{1}{S(k)}\right]. \tag{31}$$

Another static characteristic we employed was the static value of the DSF, $S(k,0)$. Since the asymptotic behavior of the DLFC as $\omega \to 0$ is difficult to predict for strongly coupled systems, we had to consider $S(k,0)$ to be an input parameter determined on the basis of the simulation data together with the SSF $S(k)$.

The influence of the SLFC on the static properties of dense and cold electronic liquids (the interaction potential, the static conductivity, etc.) within the STLS model [14] has recently been studied in detail in [24].

It follows from Eq. (25) that $A(k,\omega \to \infty) \simeq -U(k)$ asymptotically. Thus, we recover the VEA, which is an interpolation between the asymptotic values of the DLFC at $\omega = 0$ and $\omega \to \infty$:

$$G^{VEA}(k,\omega) = \frac{B(k,0) - i\tau\omega A(k,\infty)}{1 - i\tau\omega} = \frac{G(k) + i\tau\omega U(k)}{1 - i\tau\omega}. \tag{32}$$

But expression (28) might be considered as an extension of the VEA equivalent to representation (17) and

$$\epsilon^{-1}(k,\omega) = 1 + \frac{\omega_p^2(\omega\tau + i)}{\omega\tau(\omega^2 - \omega_2^2) + i(\omega^2 - \omega_1^2)}, \tag{33}$$

stemming from Eq. (22) with $Q = i\tau^{-1}$ [25]. As further shown in Sec. V, numerical results obtained from Eqs. (17) and (33) coincide, within the computational error, with those found from Eqs. (26)–(28).

It is relevant to note that the model expression for the DSF [Eq. (17)] coincides formally with that obtained within the same VEA in [22]. Such a coincidence takes place because the adjustable parameters of the general hydrodynamics approach [22] were chosen to satisfy the same number of convergent frequency moments of the DSF. The difference between these two expressions lies in that the OCP hydrodynamic characteristics, which, of course, describe the dissipation processes in the system, acquire, within the moment approach, some specific definitions, see below, [Eq. (42) and (43)].

Generally speaking, the hydrodynamic characteristics such as the kinematic viscosity, the adiabatic sound velocity, and the thermal conductivity, for which there exist generic expressions in terms of the specific limiting values of the correlation functions of the hydrodynamic current longitudinal component, can presumably be determined by numerical simulations only.

The choice of the Nevanlinna parameter function, a nonphenomenological component of the moment approach, might seem to be as arbitrary as that of the memory function form and its parameters, see, e.g., [22]. Nevertheless, here we manage to relate all parameters involved in Eq. (17) to measurable quantities such as the zero-frequency value of the DSF. Although, for more realistic systems such as two-component plasmas [16], the Nevanlinna parameter function can further be specified by taking into account some details of the energy dissipation processes [17].

B. Remark on the continued-fraction approach

As it is mentioned above, we compare our theoretical results to two data sets [3,10]. The theoretical approach employed in [3] was the method of recurrence relations [15], closely related to the method of continued fractions, which, in turn, is equivalent to the classical moment method we apply. Indeed, it is easy to see that expression (22) for the response function

$$\chi(k,z) = \epsilon^{-1}(k,z) - 1 = \frac{\omega_p^2(z + Q)}{z(z^2 - \omega_2^2) + Q(z^2 - \omega_1^2)}, \quad z = \omega + i0^+ \tag{34}$$

is equivalent to the truncated continuous-fraction form [3] (the so-called J-fraction, for a recent review, see [26]):

$$\chi(k,z) \coloneqq \epsilon^{-1}(k,z) - 1 = \chi(k,0)\left(1 - \cfrac{z}{z - \cfrac{\omega_1^2}{z - \cfrac{\omega_2^2 - \omega_1^2}{z + Q}}}\right) \tag{35}$$

with the same Nevanlinna parameter function $Q = Q(k,z)$, $\chi(k,0) = \epsilon^{-1}(k,0) - 1$. Of course, representation (35) satisfies

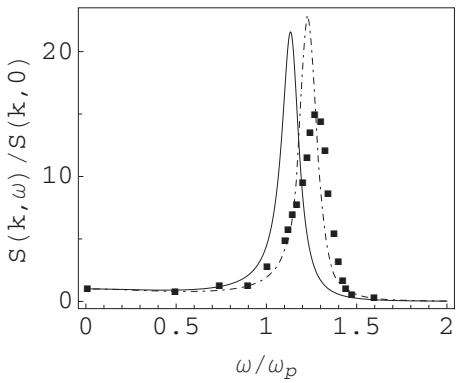

FIG. 1. The OCP normalized dynamic structure factor for $\Gamma=0.993$ and $q=0.6187$ in comparison with the simulation data of [10] (boxes). The solid line is constructed according to Eq. (17) with the values of the moments taken from [10] and/or calculated by the HNC method; the dot-dashed line is also constructed according to Eq. (17) but with the values of the moments obtained by direct integration of the graphic data of [10].

the sum rules (21) independently of the choice of the function $Q=Q(k,z)$. Nevertheless, the form of the DLFC employed in [3], is equivalent to the VEA expression (32) but without any limitation to small wavelengths.

IV. PLASMA MODES

A. Approximate solution to the dispersion relation

If, in a complete accord with the Landau damping, the decay rate of the plasma mode is assumed exponentially small, then, the poles of Eq. (33) lead to the existence of two modes in the system, i.e., the diffusion, unshifted, mode at $\omega_{us}=0$ and the plasmon modes at $\omega_L=\pm\omega_2(k)$. From the mathematical point of view, such an assumption implies the incorporation of the so-called canonical solution to the moment problem [27] for the DSF:

$$S(k,\omega)=\omega_0^2\left\{\left(\frac{1}{\omega_1^2}-\frac{1}{\omega_2^2}\right)\delta(\omega)+\frac{1}{2\omega_2^2}[\delta(\omega+\omega_2^2)+\delta(\omega-\omega_2^2)]\right\}, \tag{36}$$

which generalizes the Feynman approximation for the DSF

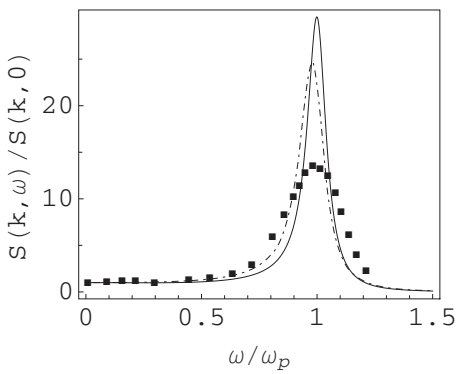

FIG. 2. Same as in Fig. 1 but for $\Gamma=9.7$ and $q=1.3835$.

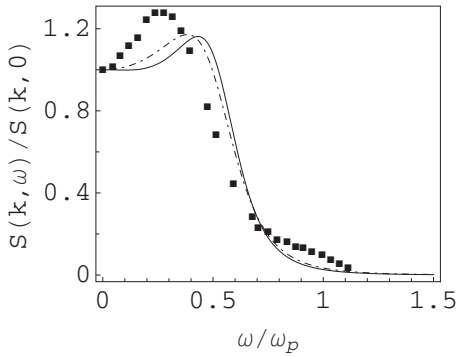

FIG. 3. Same as in Fig. 1 but for $\Gamma=110.4$ and $q=3.0937$.

used in [22] (Chap.7) and, thus, justifies the VEA.

Equation (36) makes the Landau-Placzek ratio,

$$R_{LP}(k)=\frac{\omega_2^2-\omega_1^2}{\omega_1^2}>0,$$

a measurable quantity. Note that if the plasma isothermal compressibility is introduced as $\kappa=n(\partial n/\partial p)_\beta$, with p being the pressure, the compressibility sum rule then states that

$$G(k\to 0)=\frac{k^2}{k_D^2}\left(1-\frac{\beta n}{\kappa}\right), \tag{37}$$

hence, due to Eq. (8),

$$R_{LP}(k\to 0)\simeq\frac{k^2}{k_D^2}\left(3-\frac{n\beta}{\kappa}+\frac{8\pi k_D^2}{15k_0^2}\right). \tag{38}$$

On the other hand, in the classical limit one gets for any frequency,

$$\lim_{k\to\infty}G(k,\omega)=1-g(0)=1, \tag{39}$$

$$R_{LP}(k\to\infty)\simeq 2. \tag{40}$$

Further, if the decay decrements are assumed to be finite but small enough, then, the dispersion relation

$$\omega\tau(\omega^2-\omega_2^2)+i(\omega^2-\omega_1^2)=0 \tag{41}$$

can approximately be solved to give simple estimates for the decrements of the two collective modes, respectively, as

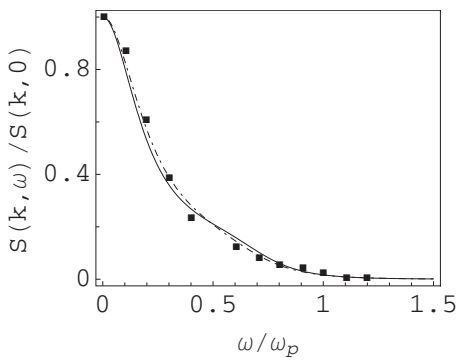

FIG. 4. Same as in Fig. 1 but for $\Gamma=152.4$ and $q=6.1837$.

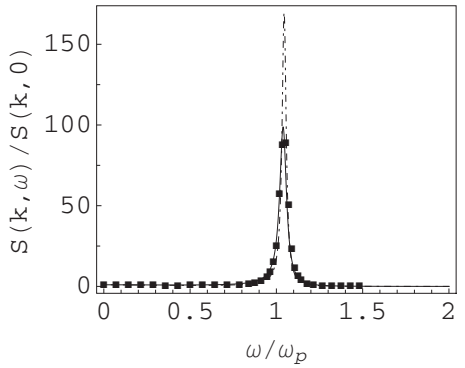

FIG. 5. The OCP normalized dynamic structure factor for $\Gamma=2.0$ and $q=0.49109$ in comparison with the simulation data of [3] (boxes). The solid line is constructed according to Eq. (17) with the values of the moments taken from [3] and/or calculated by the HNC method; the dot-dashed line is also constructed according to Eq. (17) but with the values of the moments obtained by direct integration of the graphic data of [3].

$$\delta_{us}(k) = -\frac{\omega_1^2(k)}{\tau(k)\omega_2^2(k)}, \tag{42}$$

$$\delta_L(k) = -\frac{\omega_p^2\Delta(k)}{2\tau(k)\omega_2^2(k)}. \tag{43}$$

Both decrements determined above are obviously negative.

Finally, by construction, the sum of the intensities of all three peaks equals $S(k)$, i.e., satisfies the *elastic sum rule.*

One serious drawback of the above approximate solution to the dispersion equation is that it is unable to predict the appearance of the "negative" dispersion, i.e., physical conditions under which the derivative $d\omega_L(k)/dk$ first vanishes and, then, turns negative. To specify these conditions it is necessary to study the dispersion relation in a stricter manner.

B. Exact solution of the dispersion relation

Dispersion relation (41) can be solved exactly using the Cardano formulas. Let $w=\exp(\frac{2\pi i}{3})=(-\frac{1}{2}+\frac{1}{2}i\sqrt{3})$ and introduce the following parameters:

$$Z^3 = \sqrt{-\left(\frac{\omega_2^2}{3}-\frac{1}{9\tau^2}\right)^3 - \frac{1}{4\tau^2}\left(-\frac{\omega_2^2}{3}+\omega_1^2+\frac{2}{27\tau^2}\right)^2},$$

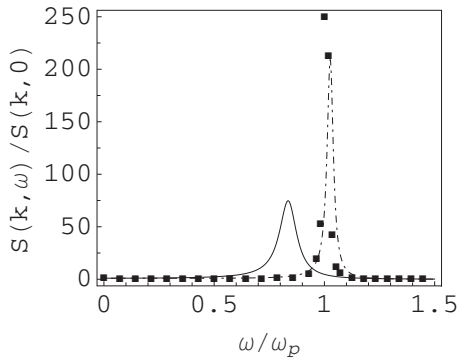

FIG. 6. Same as in Fig. 5 but for $\Gamma=4.0$ and $q=0.34725$.

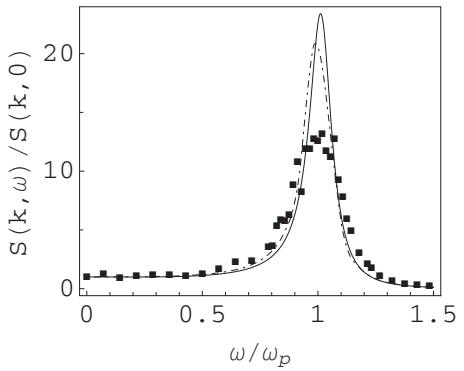

FIG. 7. Same as in Fig. 5 but for $\Gamma=8.0$ and $q=1.389$.

$$X = \sqrt[3]{Z^3 - \frac{i}{2\tau}\left(-\frac{\omega_2^2}{3}+\omega_1^2+\frac{2}{27\tau^2}\right)},$$

$$Y = \sqrt[3]{-\frac{i}{2\tau}\left(-\frac{\omega_2^2}{3}+\omega_1^2+\frac{2}{27\tau^2}\right) - Z^3}.$$

Then, the exact solutions of the dispersion relation, i.e., the solution with the zero real part and two solutions with symmetric real parts, are

$$\omega_{us} = -w^2X - wY - \frac{i}{3\tau}, \tag{44}$$

$$\omega_L = -wX - w^2Y - \frac{i}{3\tau}, \tag{45}$$

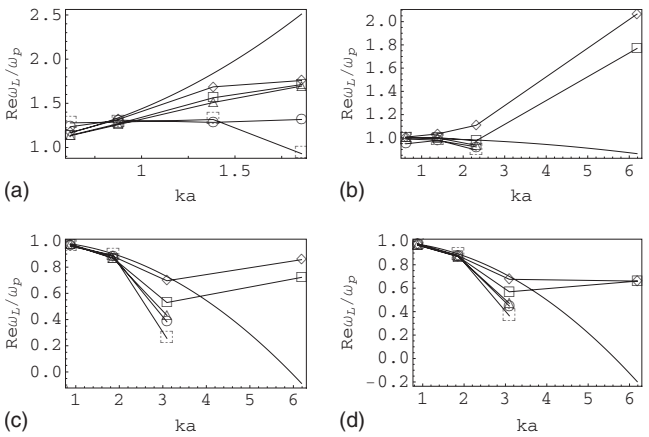

FIG. 8. The normalized plasmon frequency Re $\omega_L(q)/\omega_p$ for four different values of Γ: (a) $\Gamma=0.993$; (b) $\Gamma=9.7$; (c) $\Gamma=110.4$; and (d) $\Gamma=152.4$. Solid lines: VEA [Eq. (50)]; diamonds: the approximate solution of the dispersion equation, Re $\omega_L(q)/\omega_p=\omega_2(q)/\omega_p$; triangles: determined from the positions of the reconstructed DSF maxima with the values of the moments taken from [10]; circles: same as triangles but with the values of the moments obtained by direct integration of the graphic data of [10]; squares: the exact solution of the dispersion equation with the values of the parameters taken from [10]; dashed squares: determined from the positions of DSF maxima of the graphic data of [10].

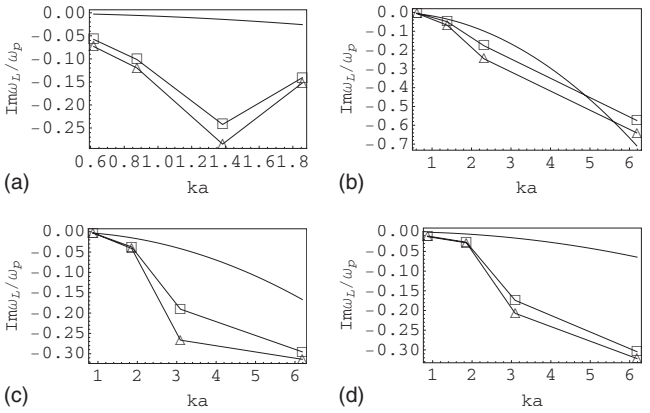

FIG. 9. The normalized plasmon decay rate Im $\omega_L(q)/\omega_p$ for four different values of Γ: (a) $\Gamma=0.993$; (b) $\Gamma=9.7$; (c) $\Gamma=110.4$; and (d) $\Gamma=152.4$. Solid lines: VEA [Eq. (50)]; triangles: the approximate solution of the dispersion equation (51); squares: the exact solution of the dispersion equation calculated using the data of [10].

$$\omega_L' = -X - Y - \frac{i}{3\tau}. \tag{46}$$

The approximate solutions are naturally recovered

$$\omega_{us}(k) \simeq -\frac{i\omega_1^2(k)}{\tau(k)\omega_2^2(k)}, \tag{47}$$

$$\omega_L(k) \simeq \omega_2(k) - \frac{i\omega_p^2\Delta(k)}{2\tau(k)\omega_2^2(k)}, \tag{48}$$

$$\omega_L'(k) \simeq -\omega_2(k) - \frac{i\omega_p^2\Delta(k)}{2\tau(k)\omega_2^2(k)} \tag{49}$$

when, formally, $\tau(k)\to\infty$.

It is expected that the frequencies $\omega_L(k)$ [and $\omega_L'(k)$] correspond to the positions of the shifted peaks of the DSF [1].

Our results for the OCP collective modes are invalid in the long-wavelength limit only like those, for instance, of the VEA hydrodynamic approach [22]. Note that in the QLCA

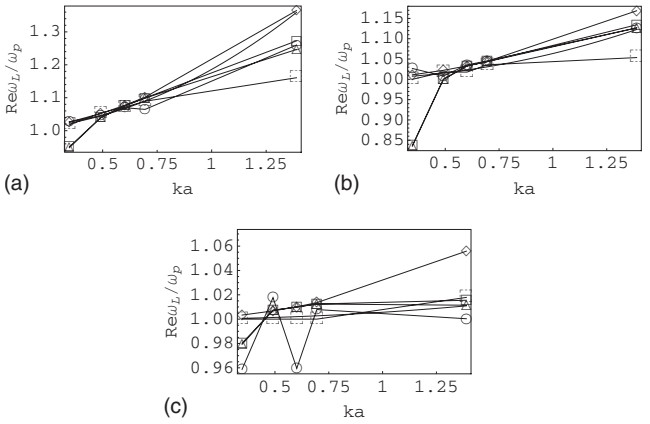

FIG. 10. Same as in Fig. 8 but using the data of [3] for three different values of Γ: (a) $\Gamma=2$; (b) $\Gamma=4$; and (c) $\Gamma=8$.

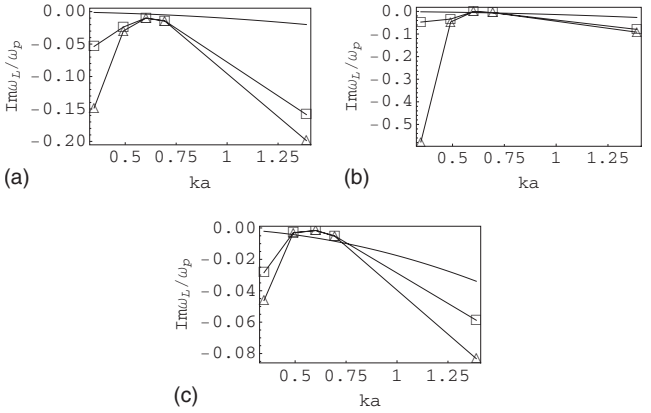

FIG. 11. Same as in Fig. 9 but using the data of [3], for three different values of Γ: (a) $\Gamma=2$; (b) $\Gamma=4$; and (c) $\Gamma=8$.

the direct thermal effects are dropped out, i.e., the corresponding dispersion relation for the plasmon mode lacks the classical Vlasov contribution [11], [12] (though in [19] this contribution was included as a result of the moment analysis without providing any detail or obtaining quantitative agreement with the simulation data) and the decrements of the collective modes are out of the scope of that theory.

V. NUMERICAL RESULTS AND DISCUSSION

We have carried out a numerical analysis of the dispersion relation (45) based on the HNC results for the static characteristics and have confirmed that the derivative $d\omega_L(k)/dk$ vanishes at about $\Gamma=9$ so that the negative dispersion takes place for higher values of the coupling parameter Γ.

We have also carried out an extensive comparison of our theoretical results with the simulation data of [3,10]. To do so we have used the graphic data presented in [10] and the numerical data of [3].

First of all we compare the theoretically predicted and simulated forms of the DSF (Figs. 1–7). The simulation data have been processed in two different ways to calculate the static parameters [the frequencies $\omega_j^2(k)$, $j=1,2$, etc.]. We

TABLE I. The values of $S(q=ka,0)$ taken from [10].

	$q=0.6187$	$q=0.8750$	$q=1.3835$	$q=1.8562$
$\Gamma=0.993$	0.0133	0.0413	0.1059	0.1581
	$q=0.6187$	$q=1.3837$	$q=2.315$	$q=6.1873$
$\Gamma=9.7$	0.001	0.0075	0.0763	0.3897
	$q=0.8750$	$q=1.8562$	$q=3.0937$	$q=6.1873$
$\Gamma=110.4$	0.0003	0.0045	0.1220	1.003
	$q=0.8750$	$q=1.8562$	$q=3.0937$	$q=6.1873$
$\Gamma=152.4$	0.0001	0.0045	0.1160	1.0733

TABLE II. The values of $S(q=ka,0)$ taken from [3].

	$q=0.34725$	$q=0.8750$	$q=1.3835$	$q=1.8562$	$q=1.8562$
$\Gamma=0.5$	0.007897	0.025195	0.040043	0.055783	0.145137
$\Gamma=1$	0.002741	0.005957	0.022131	0.029141	0.097899
$\Gamma=2$	0.001305	0.002572	0.013369	0.018699	0.059578
$\Gamma=4$	0.000665	0.001557	0.011154	0.015553	0.036259
$\Gamma=8$	0.000256	0.000509	0.001203	0.001343	0.009562

have used either the static MD data presented in the above mentioned papers, or the data on the DSF itself to calculate the moments directly. In the latter case, care, of course, has been taken of the "tails" of the DSF, corresponding to high frequencies: the asymptotic behavior of the DSF according to Eq. (4) has been used, in a consistent way, to evaluate the high-frequency contributions to the moments.

In all figures below we display the dimensionless DSF normalized to its zero-frequency value, $S(k,\omega)/S(k,0)$, vs the dimensionless frequency ω/ω_p at fixed values of the dimensionless wave numbers $q=ka$ and at different values of the coupling parameter Γ, corresponding to the OCP liquid state. It is seen that a good quantitative agreement with the simulation data is gained, especially, for the positions of the unshifted peaks of the DSF, i.e., for the plasmon mode dispersion when the moments are calculated by direct integration of the DSF data.

In a few cases we have had to adjust the static values of the DSF within the numerical precision. In this context it is necessary to admit that the simulation data of [10], which are already 34 years old, proved to be somewhat inconsistent when we used the graphic data of [10] on the DSF to estimate the values of the power moments $\{S_\nu(k)\}_0^4$. They turn out quite different from the corresponding values provided in the paper.

Additionally, we present results for the dispersion relation of the Langmuir mode and the corresponding decay rates obtained by the exact and approximate solutions of the dispersion equation $\epsilon(k,\omega)=0$ (Figs. 8–11). These results on the dispersion are compared to the positions of the plasmon peaks of the DSF and to the prediction of the VEA estimate [28],

$$\frac{\omega_L(q)}{\omega_p} = 1 + \frac{q^2}{2\Gamma}\left(1+\frac{\delta_1}{3}\right) + i\delta_2\frac{q^2}{6\Gamma},$$

$$\delta_1 = -\frac{6\Gamma}{25} - \frac{4\Gamma}{25}W_1(0.23\sqrt{\Gamma}),$$

$$\delta_2 = -\frac{4\Gamma}{25}W_2(0.23\sqrt{\Gamma}), \tag{50}$$

where

$$W(\xi) = W_1(\xi) + iW_2(\xi) = 1 + \frac{\xi}{\sqrt{2}}Z\left(\frac{\xi}{\sqrt{2}}\right),$$

and $Z(x)$ is defined in Eq. (23) [23].

Notice that no plasmon mode is observed on Fig. 4 for $\Gamma=152.4$ and $q=6.1837$. This is confirmed by our exact solution of the dispersion relation with the module of the imaginary part being only about a half of the real part of the solution, see Figs. 8 and 9(d).

Regarding the existence of negative dispersion due to interparticle correlations, we should note that the comparison of simulations results obtained in Refs. [3,10] is not conclusive at this point, since both show quantitatively different trends at large values of Γ. But even in the case of [3], we observe that the correlational energy term amounts to compensate the Vlasov thermal dispersion contribution at the highest value of the coupling. Nonetheless, we should outline here the good agreement achieved in any case by our theoretical approach, once the static characteristics have been computed through numerical simulations. We should also mention that the accuracy of our calculations for the dispersion in Fig. 10(c) might be affected by the fact that the maximum frequency available in the simulated spectra in [3] only reaches a value of 2.8 (compared to 6.5 for the other two cases). This might be applicable especially for the circles line in Fig. 10(c).

Within our approach we can also compute the effects of damping processes on the collective mode, which is given by the imaginary part of the zeros of the dispersion equation $\epsilon(k,\omega)=0$. Our results show an increment of the modulus of the imaginary part of those zeros, as a function of k. This behavior is expected due to the existence of the well-known Landau damping mechanism, which dominates at those higher values of the wave vector. There are two additional main damping mechanisms, namely, collisional damping and diffusional damping. The latter is more relevant at small values of k. Figure 11 points out the fact that there is a certain nonmonotonic behavior of the damping as a function of k, which could be explained by a cancellation of those damping mechanisms at intermediate values of the wave number. In addition, we observe that higher values of the coupling parameter tend to counteract damping effects, probably due to the higher particle localization. Finally, it is evident that the usage of the VEA tends to underestimate notably the importance of damping processes. Again, this is not surprising, as this approximation does not describe dynamical screening adequately at intermediate frequencies. Finally, for the reference, we present the values of the static parameter $S(q=ka,0)$ we used in the present work, see Tables I and II.

VI. CONCLUSIONS

In conclusion, a fairly good agreement is obtained with numerous simulation data on the dynamic properties of

strongly coupled one-component plasmas. The model expressions for the DSF or the DLFC characteristic for the VEA or the recurrence relation approach are incorporated into the moment scheme. This allows us to determine the abstract component of our approach based on phenomenologically sounded properties. Our results on the collective modes and their damping complement those found with other approaches. A more systematic set of simulation of this system could be interesting with the aim of studying the onset of negative dispersion and quantitative damping properties at long wavelengths. Our methods can be used to model dynamic properties of more complex Coulomb systems with high density of energy.

ACKNOWLEDGMENTS

The authors acknowledge the financial support of the Spanish Ministerio de Educación y Ciencia Project No. ENE2007-67406-C02-02/FTN, the Foundation of the First President of the Republic of Kazakhstan, the Al-Farabi Kazakh National University, and ESF.

[1] S. Ichimaru, Rev. Mod. Phys. **54**, 1017 (1982); M. Baus and J.-P. Hansen, Phys. Rep. **59**, 1 (1980).
[2] K. I. Golden and G. J. Kalman, Phys. Plasmas **7**, 14 (2000).
[3] A. Wierling, T. Pschiwul, and G. Zwicknagel, Phys. Plasmas **9**, 4871 (2002).
[4] S. Alexander, P. M. Chaikin, P. Grant, G. J. Morales, P. Pines, and D. Hone, J. Chem. Phys. **80**, 5776 (1984); K. Kremer, M. O. Robbins, and G. S. Grest, Phys. Rev. Lett. **57**, 2694 (1986).
[5] S. L. Gilbert, J. J. Bollinger, and D. J. Wineland, Phys. Rev. Lett. **60**, 2022 (1988); M. G. Raizen, J. M. Gilligan, J. C. Bergquist, W. M. Itano, and D. J. Wineland, Phys. Rev. A **45**, 6493 (1992); D. H. E. Dubin and T. M. O'Neill, Rev. Mod. Phys. **71**, 87 (1999).
[6] S. Ichimaru, Rev. Mod. Phys. **65**, 255 (1993); *The Equation of State in Astrophysics*, edited by G. Chabrier and E. Schatzman (Cambridge University Press, Cambridge, 1994).
[7] H. Ohta and S. Hamaguchi, Phys. Rev. Lett. **84**, 6026 (2000); G. Kalman, M. Rosenberg, and H. E. DeWitt, *ibid.* **84**, 6030 (2000); P. K. Kaw and A. Sen, Phys. Plasmas **5**, 3552 (1998); M. S. Murillo, Phys. Rev. Lett. **85**, 2514 (2000).
[8] V. M. Adamyan and I. M. Tkachenko, *Dielectric Conductivity of Nonideal Plasmas*, Lectures on Physics of Nonideal Plasmas: Part I (Odessa State University, Odessa, 1988) in Russian; V. M. Adamyan and I. M. Tkachenko, Contrib. Plasma Phys. **43**, 252 (2003).
[9] S. V. Adamjan and I. M. Tkachenko, Ukr. J. Phys. **36**, 1336 (1991) (in Russian) [English translation is available on request imtk@mat.upv.es]
[10] J.-P. Hansen, I. R. McDonald, and E. L. Pollock, Phys. Rev. A **11**, 1025 (1975).
[11] G. Kalman and K. I. Golden, Phys. Rev. A **41**, 5516 (1990).
[12] K. I. Golden, G. Kalman, and Ph. Wyns, Phys. Rev. A **46**, 3454 (1992).
[13] S. Tanaka and S. Ichimaru, Phys. Rev. A **35**, 4743 (1987).
[14] S. Ichimaru, *Statistical Plasma Physics: Condensed Plasmas* (Addison-Wesley, New York, 1994), Vol. 2.
[15] J. Hong and M. H. Lee, Phys. Rev. Lett. **55**, 2375 (1985); J. Hong and C. Kim, Phys. Rev. A **43**, 1965 (1991).
[16] Yu. V. Arkhipov, A. Askaruly, D. Ballester, A. E. Davletov, G. M. Meirkanova, and I. M. Tkachenko, Phys. Rev. E **76**, 026403 (2007).
[17] V. I. Perel' and G. M. Eliashberg, Zh. Eksp. Teor. Fiz. **41**, 886 (1961) [Sov. Phys. JETP **14**, 633 (1962)].
[18] N. I. Akhiezer, *The Classical Moment Problem* (Hafner, New York, 1965).
[19] M. Minella and G. Kalman, in *Strongly Coupled Plasma Physics*, edited by F. H. Rogers and H. E. DeWitt (Plenum, New York, 1987), pp. 483–489.
[20] M. G. Krein and A. A. Nudel'man, *The Markov moment problem and extremal problems*, Translations of Mathematical Monographs (American Mathematical Society, Providence, RI, 1977), Vol. 50.
[21] Notice that the polynomials $\{D_j(\omega;k)\}_0^\infty$ can be obtained from the canonical basis $\{1,\omega,\omega^2,\ldots\}$ by the Gramm-Schmidt procedure with the scalar product in the vector space of (real) polynomials defined as $\langle f,g\rangle=\int_{-\infty}^{\infty}f(\omega)g(\omega)S(k,\omega)d\omega$.
[22] J.-P. Hansen and I. R. McDonald, *Theory of Simple Liquids* (Academic Press, New York, 1976).
[23] J. D. Huba, NRL Plasma Formulary, Naval Research Laboratory, Washington, DC, 2007; http://wwwppd.nrl.navy.mil/nrlformulary/NRL_FORMULARY_07.pdf
[24] K. Bennadji, M.-M. Gombert, and A. Bendib, Phys. Rev. E **79**, 016408 (2009).
[25] Observe that Eq. (32) coincides with Eq. (2.159) of [14] if we identify the Nevanlinna static parameter $\tau(k)$ as the generalized viscoelastic relaxation time $\tau_m(k)$ and observe that by Eq. (2.146) of [14], $U(k)=-I(k)$.
[26] G. Valent and W. Van Assche, J. Comput. Appl. Math. **65**, 419 (1995).
[27] I. M. Tkachenko, *Book of Abstracts of the International Conference on Operator Theory and Applications in Mathematical Physics* (Stefan Banach International Mathematical Center, Będlewo, 2002), p. 20.
[28] J.-P. Hansen, J. Phys. Lett. **42**, 397 (1981).